



## Synthesis of Nanocrystalline of Lanthanum Doped NaTaO<sub>3</sub> and Photocatalytic Activity for Hydrogen Production

Husni Husin<sup>1,2\*</sup>, Komala Pontas<sup>1,2</sup>, Yuliana Sy<sup>1</sup>, Syawaliah<sup>1</sup> & Saisa<sup>2</sup>

<sup>1</sup> Department of Chemical Engineering, Syiah Kuala University

<sup>2</sup> Graduate Study of Chemical Engineering, Syiah Kuala University  
Jalan Tgk. Syeh Abdurrauh No. 7, Darussalam, Banda Aceh 23111, Indonesia

\*Email: husni\_husin2002@yahoo.com

**Abstract.** Sodium tantalum oxide doping lanthanum (La-NaTaO<sub>3</sub>) compounds were successfully synthesized by a sol-gel method and calcined at different temperatures. Tantalum chloride (TaCl<sub>5</sub>) was used as starting material and lanthanum nitrate (La(NO<sub>3</sub>)<sub>3</sub>·6H<sub>2</sub>O) as lanthanum source. X-ray diffraction (XRD) revealed that the calcination temperature strongly influenced the crystallinity of the prepared samples. The crystallite sizes of the resultant La-NaTaO<sub>3</sub> were in the range of 27-46 nm. The photocatalytic activities of the samples were examined for hydrogen production from an aqueous methanol solution under UV light irradiation. It was found that the photocatalytic activity of the La-NaTaO<sub>3</sub> depended strongly on the calcination temperature. The range of calcination temperatures were 500, 700, and 900°C. The La-NaTaO<sub>3</sub> sample calcined at 900°C showed the highest photocatalytic activity compared to the samples calcined at the other temperatures. The rate of hydrogen production reached a value of 6.16 mmol h<sup>-1</sup> g<sup>-1</sup> catalyst.

**Keywords:** green energy; hydrogen; La-doped NaTaO<sub>3</sub>; photocatalyst; sol-gel.

### 1 Introduction

The delivery of massive energy from fossil fuels produces an energy crisis and environmental pollution. This makes it necessary to develop non-polluting and renewable energy sources [1]. Hydrogen is an ideal source of clean energy as well as a raw material for many chemical industries. Hydrogen, a clean energy carrier, should not be produced from irreproducible fossil fuels but from renewable resources [2]. Currently, hydrogen is mainly produced by reforming petroleum and natural gas at a high temperature, which consumes a huge amount of energy [3]. Thus, the development of an alternative hydrogen production method is absolutely imperative in order to reduce environmental impact and prevent energy issues [4].

Photocatalytic water-splitting is the most promising approach, because it can be carried out at room temperature, using semiconductors and solar light as the source of photons ( $h\nu$ ). A large area should be used, in order to harvest a

reasonable amount of solar energy. Photocatalytic water-splitting is advantageous for large-scale application of solar hydrogen production because of its simplicity [5]. It is the most promising technology for this purpose, as through this process  $H_2$  can be obtained directly from abundant and renewable water and solar light [6]. Since the discovery of hydrogen evolution over a  $TiO_2$  single crystal electrode [7], the technology of semiconductor-based photocatalytic water-splitting to produce hydrogen using solar energy is considered one of the most important approaches to solving the world energy crisis [8].

The principle of photocatalytic decomposition of water using a semiconductor photocatalyst are: (a) a semiconductor photocatalyst have a valence band (VB) and a conduction band (CB); (b) when photons of light interact with the semiconductor, lead to the formation of electrons ( $e^-$ ) in the conduction band and holes ( $h^+$ ) in the valence band; (c) Hydrogen ions ( $H^+$ ) is generated by interaction of holes with electron donors, i.e. in the case of water-alcohol mixtures, with both water and alcohol [9]. Simultaneously, the electrons generated reduce the hydrogen ions to hydrogen gas. When alcohol presence in the solution, its can act as a sacrificial electron donor and consume photogenerated holes to produce more protons ( $H^+$ ) in the valence band, thereby suppressing the rate of electron-hole recombination and back reaction between hydrogen and oxygen [2].

The study of photocatalytic water-splitting has focused on the development of various semiconductor materials, including:  $TiO_2$  [10],  $ZnO/ZnS$  [11], and  $NaTaO_3$  [12]. Among them,  $NaTaO_3$  photocatalyst has the highest photocatalytic activity for hydrogen production [13].  $NaTaO_3$ -based photocatalyst, such as  $La_{0.02}NaTaO_3$ ,  $SmNaTaO_3$ , and  $N-NaTaO_3$ , have been reported to act as efficient photocatalysts to split water into  $H_2$  and  $O_2$  under UV light irradiation [14]. In previous publications it was reported that the photocatalytic activity increased after  $NaTaO_3$  was doped with lanthanum [15].

The photocatalytic efficiency of  $NaTaO_3$  has some limitations due to the recombination rate of the photo-generated electron-hole pairs. To resolve this issue and enhance the photocatalytic activity of the photocatalyst, various approaches have been employed, including doping the semiconductors with other impurities [16] and optimization of reaction conditions by setting the calcination temperature [17] in order to improve the crystallinity of the material. However, the effects of the calcination temperature on the morphology and photocatalytic activity of  $La-NaTaO_3$  have not yet been reported. Meanwhile, many studies have confirmed that the photocatalytic activity of semiconductors is strongly influenced by the calcination temperature [18].

Hence, in the present work, we have investigated the effect of the calcination temperature on the growth of crystallite size of La-NaTaO<sub>3</sub> catalyst and the photocatalytic properties of La-NaTaO<sub>3</sub> via the photocatalytic activity of hydrogen production from a methanol/water solution. The catalyst was prepared by a sol-gel method using ethanol and water as solvent. To evaluate the characteristics of the sample, the NaTaO<sub>3</sub> was analyzed by powder X-ray diffraction (XRD).

## 2 Experimental Procedure

### 2.1 Catalyst Preparation

Analytical grade sodium hydroxide (Acros, ACS grade), ethanol (Acros, 99.5%), tantalum chloride (Acros, 99.9%), lanthanum nitrate (Merck, 98.0%), citric acid (Across, 99.0%), ammonium solution (35% Fisher Scientific), and methanol (Acros, 99.9% HPLC grade) were used without further purification. All solutions were prepared using high-purity deionised water. Nitrogen gas (N<sub>2</sub>) and oxygen gases (O<sub>2</sub>) were used for catalyst treatment, and argon (Ar) for purging and as GC carrier gas. All gases were purchased from Serikat Company Banda Aceh, Indonesia. Hot plate, stirrer, oven, pH meter, furnace, crucible, mortar, thermometer, desiccators, glass reactor, thermocouples, cooling circulation, a set of glass ware, and an Hg lamp ( $\lambda = 250\text{-}350\text{ nm}$ ) were used for catalyst preparation and photocatalyst testing.

In this work, the catalyst was prepared by dissolving TaCl<sub>5</sub> solution into 50 mL of ethanol [19], while NaOH and La(NO<sub>3</sub>)<sub>3</sub>.6H<sub>2</sub>O were dissolved respectively in deionised water and then mixed with a solution of TaCl<sub>5</sub>. Citric acid was dissolved in 50 mL of deionised water (in this work, the ratio of citric acid and TaCl<sub>5</sub> was 5:1). Subsequently, the citric acid solution was poured into a burette, then slowly dropped into the solution and stirred at room temperature for 1 h. The mixture was added a solution of NH<sub>3</sub> to achieve the desired pH. The next process was the conversion of a sol by heating the solution at 80°C to form a white gel. The gels were dried in an oven for 6 h at a temperature of 110°C. The powders were ground with a mortar and then transferred into a crucible for initial calcination at a temperature of 400°C for 3 h. After grinding at room temperature, samples were calcined at different temperatures, i.e. 500°C, 700°C, and 900°C, for 8 h. The resulting products were cooled down to room temperature and kept in a desiccator. The crystal structure of the samples was investigated using x-ray diffraction (Shimadzu 7500 X-ray diffractometer) with a Cu K $\alpha$  source, wavelength,  $\lambda = 0.15406\text{ nm}$ . The size of the crystal was determined by fitting the XRD pattern using the OriginPro 8 software.

## 2.2 Photocatalytic Reaction

Photocatalytic reactions for H<sub>2</sub> evolution were carried out in a gas-closed circulation system under UV light irradiation. Typically, 0.30 g photocatalyst powder was dispersed and magnetically stirred in a pyrex reaction cell containing 350 ml of an aqueous methanol solution, with a ratio of water to methanol of 90:10 v/v, irradiated with a 450 W mercury lamp. The suspensions were de-aerated with Ar gas for 30 min to prevent uptake of photo-generated electrons by dissolved oxygen before irradiation. The hydrogen evolution was collected in a gas collector. The hydrogen was identified by a gas chromatograph (Shimadzu GC-8A, thermal conductivity detector TCD, using argon as carrier gas and a packed column of molecular sieve 5A).

## 3 Result and Discussions

### 3.1 Catalyst Characterization

Samples were calcined at temperatures of 500, 700, and 900°C. XRD was used to investigate the phase structures of the samples. Figure 1 shows the XRD patterns of the as-prepared photocatalyst. It was found that the La-NaTaO<sub>3</sub> photocatalysts that were synthesized through the sol-gel route had crystallized well. All of the x-ray diffraction peaks could be indexed to an orthorhombic structure in good agreement with the diffraction pattern of pure NaTaO<sub>3</sub> (JCPDS Card: 25-0863). These results demonstrate that the introduction of La<sup>3+</sup> at different temperatures did not change the lattice structure of the NaTaO<sub>3</sub> [20]. The x-ray diffraction pattern of the sample calcined at 500°C (NaTa-500) had the same pattern as compounds of standard NaTaO<sub>3</sub>. There were very few impurities at 2θ of 40.8° in the XRD spectrum. The XRD spectra of the samples calcined at higher temperatures, 700°C (NaTa-700) and 900°C (NaTa-900), displayed a single-phase NaTaO<sub>3</sub> structure without any impurity phase, suggesting that the samples had a higher crystallinity. The intensity of the XRD pattern of the NaTa-500 was about 12000 cps. The peaks of the sample became narrow and the intensity increased to 35000 cps after heating at 700°C. These results suggest that the samples calcined at a temperature of 500°C produced NaTaO<sub>3</sub> powder with a lower crystallinity. A comparison of the XRD spectrum of NaTa-500 (Figure 1(a)) with the XRD patterns of NaTa-700 and NaTa-900 (Figures 1(b) & 1(c)) demonstrated that the increase in calcination temperature resulted in increases in intensity of the XRD spectra. These phenomena suggest the formation of a more perfect NaTaO<sub>3</sub> crystal when the catalyst was calcined at higher temperatures. The transformation of the precursor into a NaTaO<sub>3</sub> crystalline was not progressive at a temperature of 500°C.

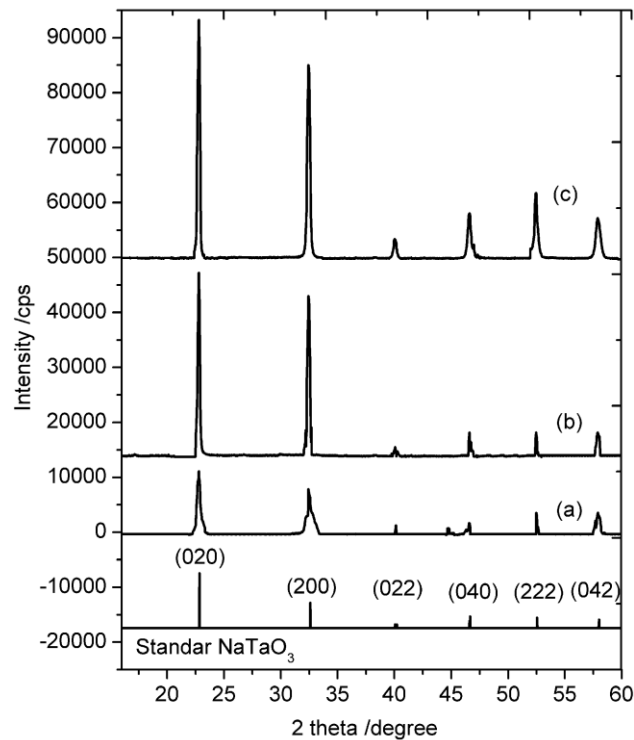


**Figure 1** XRD pattern of La-NaTaO<sub>3</sub> photocatalyst calcined at: (a) 500°C, (b) 700°C, and (c) 900°C.

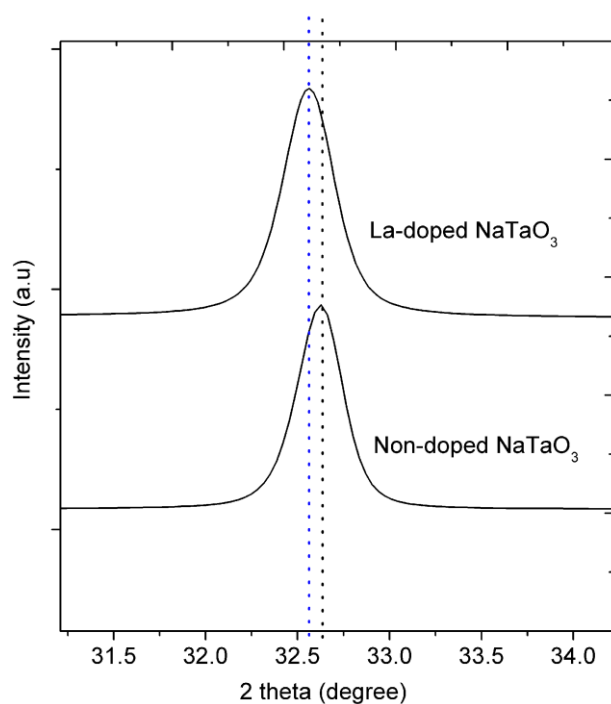
The XRD pattern was evaluated by fitting the x-ray diffraction pattern of the NaTaO<sub>3</sub> samples. Peak fitting was executed by OriginPro 8 software. The crystallite size of the particles was calculated by Scherrer's formula with the full-width at 2θ of 22.7° [21].

$$t = \frac{K * \lambda}{B * \cos \theta_B} \quad (1)$$

where B is the full width at half max (FWHM) or integral breadth in radians, t is the mean size of the crystallites (nm), K is a constant dependent on the shape of the crystal, λ is the x-ray wavelength (nm), and θ<sub>B</sub> is the Bragg angle. The crystal sizes at different calcination temperatures, as determined from the XRD data of each sample, are listed in Table 1. The powder sample calcined at 500°C exhibited a relatively small crystal size (27 nm). The crystal size increased markedly, to 41 nm, after the temperature was raised to 700°C. These results demonstrate that increasing the calcination temperature can significantly improve the crystallinity.

**Table 1** Crystallite size of La-NaTaO<sub>3</sub> photocatalyst at various temperatures.

| Temperature (°C) | Crystallite sizes (nm) <sup>a</sup> |
|------------------|-------------------------------------|
| 500              | 27                                  |
| 700              | 41                                  |
| 900              | 46                                  |

<sup>a</sup> Determined with Scherrer Equation**Figure 2** Enlarged view of XRD peak of samples at plane (200).

The same phenomenon was found at the further raised calcination temperature of 900°C, where the intensity reached up to 45000 cps. It is evident that the particle growth along with the increasing calcination temperature. High crystallinity is expected to prevent recombination between electrons and holes, thus increasing the efficiency of photocatalytic hydrogen production. Meanwhile, the rate of H<sub>2</sub> is strongly dependent on the crystallinity of the catalyst [22]. Due to operating restrictions of the equipment and the heating process, the operation could not be performed above 900°C.

To explain the existence of lanthanum in the prepared sample, an enlarged view of the peak at around  $32.5^\circ$  corresponding to plane (200) was made, as shown in Figure 2. The doped- $\text{NaTaO}_3$ , x-ray diffraction patterns of the powders were slightly shifted around  $0.15^\circ$  to lower angles. This shift indicates that at least part of the lanthanum was homogeneously doped into the  $\text{NaTaO}_3$  lattice. Similar examples have been documented in the literature, such as the effect of doping on  $\text{NaTaO}_3$  and  $\text{TiO}_2$  and their photocatalytic activity [21,23].

### 3.2 Activity of Photocatalytic of Hydrogen Production

The photocatalytic activities of the as-prepared samples were evaluated by hydrogen evolution from an aqueous methanol solution under UV light irradiation, as shown in Figure 3. Methanol was used as a sacrificial reagent.

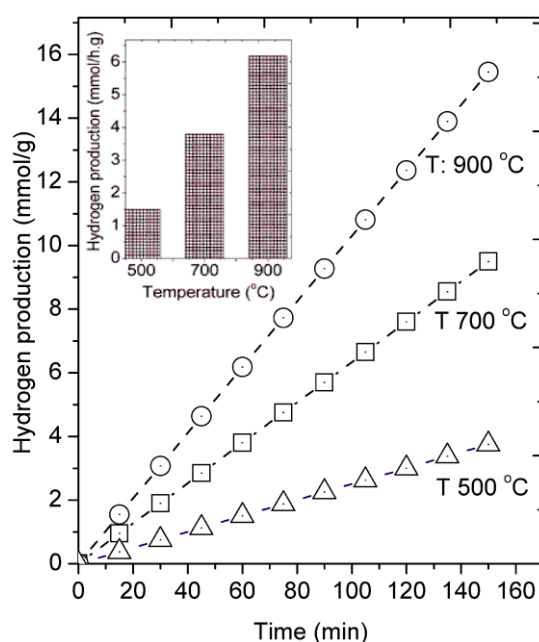


**Figure 3** Effect of calcination temperature on hydrogen production.

It is observed that the rate of hydrogen evolution increases progressively with increasing calcination temperature as well as crystallite sizes of the catalyst. The calcination temperature was an important factor affecting the photocatalytic activity of the samples. When the catalysts calcined at temperature of  $500^\circ\text{C}$ , hydrogen production of  $1.45 \text{ mmol h}^{-1} \text{ g}^{-1}$  catalyst. Starting at  $700^\circ\text{C}$ , the activity increases markedly. It is evident that the particles grow up with increase calcination temperature. The hydrogen evolution of the catalyst calcined at temperature of  $900^\circ\text{C}$  reaches up to  $6.16 \text{ mmol h}^{-1} \text{ g}^{-1}$  catalyst, suggesting its

relatively high crystallinity contributes to prevent electron-hole recombination [24].

This phenomenon can be understood because the fact that the calcination temperature can promote the growth of the crystals of the La-NaTaO<sub>3</sub> photocatalyst. This is also consistent with the crystal size of the calcined catalyst at 900°C that reaches up to 46 nm, as can be seen in Table 1. The catalyst with a high crystallinity contributed to avoid recombination between photogenerated electron-hole pairs in the bulk of photocatalyst, resulting in an increase of hydrogen evolution.

#### 4 Conclusions

Crystalline sodium tantalum oxide doped lanthanum (La-NaTaO<sub>3</sub>) catalyst samples were prepared through a sol-gel method. The La-NaTaO<sub>3</sub> samples were well-crystallized with an orthorhombic structure. The samples were calcined at different calcination temperatures. The XRD results indicate that the samples calcined at temperatures of 700°C and 900°C were well-crystallized. The crystallite sizes of the resultant La-NaTaO<sub>3</sub> were in the range of 27 to 46 nm. The rate of hydrogen evolution increased progressively with the increase of the calcination temperature of the catalyst. Hydrogen production reached a value of 6.16 mmol h<sup>-1</sup> g<sup>-1</sup> catalyst.

#### Acknowledgments

We thank the Ministry of Education and Culture of the Republic of Indonesia for financial support through the Research Grant for Doctoral and Master Program of Higher Education of Indonesia.

#### References

- [1] Moliner, R., Echegoyen, Y., Suelves, I., Lázaro, M.J. & Palacios, J.M., *Ni-Mg and Ni-Cu-Mg Catalysts for Simultaneous Production of Hydrogen and Carbon Nanofibers: The Effect of Calcination Temperature*, International Journal of Hydrogen Energy, **33**(6), pp. 1719-1728, 2008.
- [2] Lin, W.C., Yang, W.D., Huang, I.L., Wu, T.S. & Chung, Z.J., *Hydrogen Production from Methanol/Water Photocatalytic Decomposition Using Pt/TiO<sub>2</sub>-xNx Catalyst*, Energy & Fuels, **23**(4), pp. 2192-2196, 2009.
- [3] Rosen, M.A., *Advances in Hydrogen Production by Thermochemical Water Decomposition: A Review*, Energy, **35**, pp. 1068-1076, 2010.
- [4] Zheng, H.Q., Yong, H., Yang, T.O. Fan, Y.T. & Hou, H.W., *A New Photosensitive Coordination Compound [Ru(Bpy)<sub>2</sub>](PF<sub>6</sub>)<sub>2</sub> and Its Application in Photocatalytic H<sub>2</sub> Production under the Irradiation of*



- Visible Light*, International J. of Hydrogen Energy, **38**, pp. 2938-12945, 2013.
- [5] Yu, J., Qi, L. & Jaroniec, M., *Hydrogen Production by Photocatalytic Water Splitting over Pt/TiO<sub>2</sub> Nanosheets with Exposed (001) Facets*, The Journal of Physical Chemistry C, **1149**(30), pp. 13118-13125, 2010.
- [6] Boudjemaa, A., Boumaza, S., Trari, M., Bouarab, R. & Bouguelia, A., *Physical and Photo-Electrochemical Characterizations of A-Fe<sub>2</sub>O<sub>3</sub>. Application for Hydrogen Production*, Int. J. Hydrogen Energy, **34**, pp. 4268-4274, 2009.
- [7] Fujishima, A. & Honda, K., *Electrochemical Photolysis of Water at a Semiconductor Electrode*, Nature, **238**, p. 37, 1972.
- [8] Mao, S.S. & Chen, X., *Selected Nanotechnologies for Renewable Energy Applications*, International Journal of Energy Research, **31**(6-7), pp. 619-636, 2007.
- [9] Antony, R.P., Mathews, T., Ramesh, C., Murugesan, N., Dasgupta, A., Dhara, S., Dash, S. & Tyagi, A.K., *Efficient Photocatalytic Hydrogen Generation by Pt Modified TiO<sub>2</sub> Nanotubes Fabricated by Rapid Breakdown Anodization*, International J. of Hydrogen Energy, **37**, pp. 8268-8276, 2012.
- [10] Wang, Q., An, N., Bai, Y., Hang, H., Li, J., Lu, X., Liu, Y., Wanga, F., Li, Z. & Lei, Z., *High Photocatalytic Hydrogen Production from Methanol Aqueous Solution Using the Photocatalysts Cus/TiO<sub>2</sub>*, Int J Hydrogen Energy, **39**(8), pp. 1073-1079, 2013.
- [11] Sang, H. X., Wang, X.T., Fan, C.C. & Wang, F., *Enhanced Photocatalytic H<sub>2</sub> Production from Glycerol Solution over ZnO/ZnS Core/Shell Nanorods Prepared by A Low Temperature Route*, International J. of Hydrogen Energy, **37**, pp. 1348-1355, 2012.
- [12] Liu, J. W., Chen, G., Li, Z. H. & Zhang, Z. G., *Hydrothermal Synthesis and Photocatalytic Properties of ATaO<sub>3</sub> and ANbO<sub>3</sub> (A=Na and K)*, Int J Hydrogen Energy, **32**(13), pp. 2269-2272, 2007.
- [13] Liu, D.R., Jiang, Y.-S. & Gao, G.M., *Photocatalytic Degradation of an Azo Dye Using N-Doped NaTaO<sub>3</sub> Synthesized by One-Step Hydrothermal Process*, Chemosphere, **83**(11), pp. 1546-1552, 2011.
- [14] Martínez, L.M.T., Gómez, R., Cuchillo, O.V., Juárez-Ramírez, I., López, A.C. & Sandoval, F.J.A., *Enhanced Photocatalytic Water Splitting Hydrogen Production on RuO<sub>2</sub>/La:NaTaO<sub>3</sub> Prepared by Sol–Gel Method*, Catalysis Communications, **12**, pp. 268-272, 2010.
- [15] Husin, H., Su, W.N. & Hwang, B.J., *Hydrogen Production over La<sub>0.02</sub>Na<sub>0.98</sub>TaO<sub>3</sub> Photocatalysts from Pure Water and an Aqueous Methanol Solution*, Jurnal Ilmiah Sain dan Teknologi Industri, **11**(1), pp. 21-26, 2012.

- [16] Torres-Martínez, L.M., Cruz-López, A., Juárez-Ramírez, I. & Meza-de la Rosa, M.E., *Methylene Blue Degradation by NaTaO<sub>3</sub> Sol-Gel Doped with Sm and La*, Journal of Hazardous Materials, **165**(1-3), pp. 774-779, 2009.
- [17] Sun, W., Zhang, S., Wang, C., Liu, Z. & Mao, Z., *Effects of Cocatalyst and Calcination Temperature on Photocatalytic Hydrogen Evolution Over BaTi<sub>4</sub>O<sub>9</sub> Powder Synthesized by the Polymerized Complex Method*, Catal Letter, **123**, pp. 282-288, 2008.
- [18] Shi, J.W., Chen, S.H., Wang, S.M., Ye, Z.L., Wu, P. & Xu, B., *Favorable Recycling Photocatalyst TiO<sub>2</sub>/CFA: Effects of Calcination Temperature on the Structural Property and Photocatalytic Activity*, Journal of Molecular Catalysis A: Chemical, **330**, pp. 41-48, 2010.
- [19] Husin, H., Pontas, K., Meilina, H. & Hasfita, F., *Decomposition of Methanol Aqueous Solution into Hydrogen on Lanthanum doped Sodium Tantalum Oxide Semiconductor*, Journal of Chemical Engineering, University of North Sumatera, **2**, pp. 12-16, 2013.
- [20] Yan, S.C., Wang, Z.Q., Li, Z.S. & Zou, Z.G., *Photocatalytic Activities for Water Splitting of La-doped-NaTaO<sub>3</sub> Fabricated by Microwave Synthesis*, Solid State Ionics, **180**(32), pp. 1539-1542, 2009.
- [21] Husin, H., Chen, H.M., Su, W.N., Pan, C.J., Chuang, W.T., Sheu, H.S. & Hwang, B.J., *Green Fabrication of La-doped NaTaO<sub>3</sub> via H<sub>2</sub>O<sub>2</sub> Assisted Sol-Gel Route for Photocatalytic Hydrogen Production*, Appl. Catal., B: Environmental, **102**(1), pp. 343-351, 2011.
- [22] Kudo, A. & Miseki, Y., *Heterogeneous Photocatalyst Materials for Water Splitting*, Chemical Society Reviews, **38**(1), pp. 253-278, 2009.
- [23] Yao, S., Jia, X., Jiao, L., Zu, C. & Shi, Z., *La doped TiO<sub>2</sub> Hollow Fiber and their Photocatalytic Activity under UV and Visible Light*, Indian Journal of Chemistry, **51**, pp. 1049-1056, 2012.
- [24] Zhang, X., Yang, M., Zhao, J. & Guo, L. *Photocatalytic Hydrogen Evolution with Simultaneous Degradation of Organics over (CuIn)<sub>0.2</sub>Zn<sub>1.6</sub>S<sub>2</sub> Solid Solution*, International Journal of Hydrogen Energy, **38**, pp. 15985-15991, 2013